AMP-activated protein kinase stimulates osteoblast differentiation and mineralization through autophagy induction

YI LI[1,3*], JIAJIA SU[2*], WENCHAO SUN[1], LIN CAI[1] and ZHOUMING DENG[1]

[1]Department of Orthopedics, Zhongnan Hospital of Wuhan University, Wuhan, Hubei 430071;
[2]Department of Radiology, Hubei Cancer Hospital, Wuhan, Hubei 430000, P.R. China

Received December 29, 2016; Accepted January 18, 2018

DOI: 10.3892/ijmm.2018.3498

Abstract. Previous studies have reported that adenosine monophosphate-activated protein kinase (AMPK) activation can enhance osteoblast differentiation and mineralization; however, the underlying mechanism is not fully understood. Autophagy also serves an important role in osteoblast mineralization and bone homeostasis. The present study aimed to explore whether activation of AMPK could enhance osteoblast differentiation and mineralization via the induction of autophagy. The fracture healing and nonunion animal models were established and verified by X-ray imaging. Bone maturation was measured by Masson staining and the expression of AMPK, p-AMPK, microtubule-associated proteins 1A/1B light chain 3B II, and p62 in the fracture ends were detected by immunohistochemical staining. The mRNA expression levels of alkaline phosphatase (ALP), osteocalcin ,runt-related transcription factor 2 and BCN1 were determined by reverse transcription-quantitative polymerase chain reaction. 5-Bromo-4-chloro-3-indolyl phosphate/nitro blue tetrazolium staining was used to determine ALP activity and alizarin red staining was adopted to examine mineralization. Western blot analysis was performed to detect protein expression. Autophagosome was observed by Transmission electron microscopy. Small interfering (si)RNA was used to knock down the expression of target gene. *In vivo* experiments demonstrated that new bone mineralization and maturation was markedly restrained in the nonunion group, alongside decreased AMPK activation and autophagic activity, compared with in the fracture healing group. The results of an *in vitro* study indicated that AMPK activation stimulated the osteogenic differentiation of MC3T3-E1 cells, with increases in ALP activity, mineralization, and the mRNA expression levels of ALP, osteocalcin and runt-related transcription factor 2. Furthermore, AMPK activation induced autophagy, as determined by upregulation of microtubule-associated proteins 1A/1B light chain 3B, increased autophagosome density and downregulation of p62. In addition, inhibition of autophagy reversed the effects of AMPK activation on osteoblast differentiation. These results suggested that AMPK activation may stimulate osteoblast differentiation and mineralization via the induction of autophagy, and provides evidence to suggest that enhancing AMPK activation and autophagic activity may be a potential novel approach to promote fracture healing.

Correspondence to: Dr Zhouming Deng, Department of Orthopedics, Zhongnan Hospital of Wuhan University, 169 Donghu Road, Wuhan, Hubei 430071, P.R. China
E-mail: dengzhouming@foxmail.com

Present address: [3]Department of Colorectal and Anal Surgery, Zhongnan Hospital of Wuhan University, Wuhan, Hubei 430071, P.R. China

[*]Contributed equally

Key words: osteoblast, AMP-activated protein kinase, autophagy, differentiation, mineralization, fracture healing

Introduction

Osteoblasts serve an important role in bone formation and remodeling, which is active throughout life (1). It has previously been demonstrated that the differentiation of osteoblasts is likely to affect bone formation (2). Deficiencies in osteoblast differentiation and function have been reported to be involved in various pathologies, including osteoporosis, delayed bone fracture healing and osteonecrosis (3,4). Mineralization of the extracellular matrix represents the terminal stage of osteoblast differentiation and is thought to be a sign of osteoblast maturation (5).

Adenosine monophosphate (AMP)-activated protein kinase (AMPK) is a heterotrimeric complex that is comprised of a catabolic α subunit, and regulatory β and γ subunits; the isoforms of these subunits are widely expressed in various tissues, including bone (6). The activation of AMPK turns on catabolism and turns off anabolism, and it a key sensor of energy homeostasis (7). The activation of AMPK can be mediated by AMP, or its upstream kinases, including the tumor suppressor liver kinase B1 and calmodulin kinase kinase (8). Physiological stressors, including low nutrient levels, prolonged exercise or pharmacological inducers [5-aminoimdazole-4-carboxamide-1-β-D-ribofuranoside (AICAR) and metformin] can lead to the activation of AMPK. The AMPK pathway coordinates cell growth, autophagy and metabolism via transcription and direct effects on metabolic enzymes (9). Previous studies have confirmed that activation of AMPK positively regulates osteoblast differentiation and mineralization via numerous pathways, for example, by inhibition of the mevalonate

pathway and stimulation of endothelial nitric oxide synthase (eNOS) and bone morphogenetic protein (BMP)-2 expression, and by induction of Dlx5-dependent runt-related transcription factor 2 (Runx2) expression (10,11).

Autophagy refers to a cell degradation process whereby cytoplasmic materials, including aggregates, long-lived proteins and damaged organelles, are transported to lysosomes for degradation and the content is recycled (12). Autophagy has a critical role in physiological conditions, and autophagic deficiency is associated with certain diseases, including infectious diseases, cancer and neurodegeneration (13). Autophagy in osteoblasts is involved in mineralization and bone homeostasis; notably, autophagic vacuoles have been reported to act as vehicles for secretion of mineralization matrix (1). The UNC-51-like autophagy activating kinase (ULK) complex, which consists of ULK-1/2, autophagy-related protein (ATG)-13, ATG-101 and FIP200, initiates the autophagy process (14,15), and the mammalian target of rapamycin (mTOR) has been recognized as a major pathway that regulates autophagy (16). Furthermore, it has been suggested that AMPK can induce autophagy by directly activating ULK1 or via the inhibition of mTOR (9). However, the association between AMPK, autophagy, and osteoblast differentiation and mineralization remains to be fully elucidated.

The present study aimed to explore whether activation of AMPK could enhance osteoblast differentiation and mineralization via the induction of autophagy.

Materials and methods

Reagents and antibodies. AICAR (cat. no. HY-13417), compound C (cat. no. HY-13418A), 3-methyladenine (3-MA; cat. no. HY-19312) and chloroquine diphosphatase (CQ; cat. no. HY-17589) were purchased from MCE China (Shanghai, China). Ascorbic acid, β-glycerophosphatase, and reagents used in Masson staining, Alizarin red staining and electron microscopy sample processing were obtained from Sigma-Aldrich; Merck KGaA (Darmstadt, Germany). Anti-AMPKα (rabbit anti-mouse, monoclonal, cat. no. ab32047) and phosphorylated (p)-AMPKα (rabbit anti-mouse, monoclonal, cat. no. ab133448 for western blotting, and rabbit anti-mouse, polyclonal, cat. no. ab194920 for immunohistochemistry), microtubule-associated proteins 1A/1B light chain 3B (LC3B; rabbit anti-mouse, polyclonal, cat. no. ab48394), p62 (mouse anti-mouse, monoclonal, cat. no. ab56416) and β-actin (mouse anti-mouse, monoclonal, cat. no. ab8226) were purchased from Abcam (Shanghai, China).

Rabbit model of radius nonunion. A total of 24 male New Zealand white rabbits (age, 12 weeks; weight, 2.0-2.5 kg; obtained from Wuhan Wanqianjiahe Experimental Animals Co Ltd., Wuhan, China; cat. no. 42010000001221) were used in the present study. The animals were housed individually in rabbit cages under a 12-h light/dark cycle (on between 7:00 a.m. and 7:00 p.m.) with unrestricted access to food and water, and under specific pathogen-free (SPF) conditions at a constant room temperature of 22-24˚C. The animal experiments were conducted according to the National Institutes of Health Guide for the Care and Use of Laboratory Animals (17), and the present study was approved by the Wuhan University Zhongnan Hospital Research Committee (Wuhan, China). Rabbits were randomly assigned into two groups: The nonunion group and the healing group (n=12 rabbits/group). The rabbits were anesthetized with an intravenous injection of 30 mg/kg pentobarbital sodium solution. In the nonunion group, bilateral 20 mm bone defects were created in the middle portion of the radiuses. For the healing group, 10 mm bone defects were made in the middle portion of both radiuses (18,19). The normal bone was treated as the control group. The bone defects in both groups were not filled with any material (20) and the incisions were closed using 5-0 sutures. Calluses in the fracture ends were obtained from three rabbits (sacrificed prior to callus collection) every 4 weeks following surgery (4, 8, 12 and 16 weeks). After decalcification by 10% EDTA (pH 7.2-7.3) at 37˚C for 14-60 days (when the calluses became soft and could be cut using a knife), the calluses were fixed in 4% paraformaldehyde at room temperature for 24 h, embedded in paraffin, sectioned (4-mm thick sections) and examined by Masson staining and immunohistochemical staining (primary antibodies against AMPK, p-AMPK, LC3B and p62 were employed). Radiographs were captured of each forelimb 16 weeks post-operation.

Masson staining. The paraffin-embedded sections were deparaffinized and rehydrated through graded alcohol (100% for 5 min, 95% for 3 min,and 70% for 2 min), and then washed in distilled water for 2 min. Then the sections were stained in Weigert's iron hematoxylin working solution for 10 min and rinsed under running warm tap water for 5 min. The sections were then differentiated in 1% hydrochloric acid (dissolved in alcohol) for 5 sec and rinsed under running warm tap water for 5 min. The sections were then stained by xylidine ponceau and acid fuchsin solution for 4 min and rinsed under tap water for 1 min. Afterwards, the sections were differentiated in 1% phosphomolybdic acid for 5 min and spin-dried and then stained in aniline blue solution for 5 min. The sections were rinsed in 1% glacial acetic acid for 1 min and washed with distilled water. The sections were then quickly dehydrated through 95% alcohol, absolute ethyl alcohol and cleared in xylene. Finally, they were mounted with Permount™ mounting medium and observed under a Nikon E100 microscope (Nikon, Tokyo, Japan).

Immunohistochemistry. Briefly, the sections were cleared in xylene and dehydrated in ethanol. Antigen retrieval was then performed using 10 mmol/l sodium citrate buffer solution. Afterwards, endogenous peroxidase was blocked by 3% H_2O_2 for 15 min. The sections were then incubated in 10% normal goat serum followed by incubation with rabbit monoclonal (or polyclonal) primary antibody overnight at 4˚C, and incubated with horseradish-peroxidase conjugated secondary antibody (goat anti-rabbit) and washed 3 times with PBS buffer for 5 min each. DAB was added to the stain and then the slides were immersed and washed by distilled water. Finally, the sections were dehydrated in 95% ethanol, 100% ethanol, and xylene and mounted and observed under a Nikon E100 microscope (Nikon).

Cell culture. Mouse MC3T3-E1 osteoblasts (cat. no. GNM15) were purchased from Cell Bank of Chinese Academy of Sciences (Shanghai, China) and were cultured in α-minimum essential medium (Gibco; Thermo Fisher Scientific, Inc., Waltham, MA, USA) supplemented with 10% fetal bovine serum (Gibco) and 1% penicillin-streptomycin. For osteogenic differentiation and mineralization, cells were maintained in

medium supplemented with ascorbic acid (50 μg/ml) and β-glycerol phosphatase (10 mM). The medium was changed every 3 days. Cells were treated with AICAR (10 μm) in the presence or absence of 3-MA (5 mm) or CQ (10 μm) for 24 h at 37˚C. Cells in the control group were treated with PBS.

Transmission electron microscopy. After the indicated time and treatment, MC3T3-E1 cells were fixed with 2.5% glutaraldehyde in 0.1 M sodium dihydrogen phosphatase (pH 7.4) for 4 h at 4˚C and were then fixed with 1% OsO_4 for 1 h at room temperature, followed by dehydration using graded ethanol solutions and gradual infiltration with epoxy resin. Ultra-thin sections (60-80 nm) were stained with uranyl acetate and lead citrate, and were observed under a transmission electron microscope (Hitachi H-7500; Hitachi, Ltd., Tokyo, Japan). In addition, the density of autophagosomes was calculated using the following formula: Number of autophagic vacuoles/number of osteoblasts, as previously described (21); the values are presented relative to the control group.

Reverse transcription-quantitative polymerase chain reaction (RT-qPCR) analysis. The mRNA expression levels of alkaline phosphatase (ALP), osteocalcin (OCN), Runx2 and β-actin were determined by RT-qPCR using SYBR-Green. Total RNA was extracted using TRIzol® reagent (Invitrogen; Thermo Fisher Scientific, Inc.) according to the manufacturer's protocol. Subsequently, ~1 μg RNA underwent RT, in order to generate single-stranded cDNA. Total RNA (500 ng) was reverse-transcribed using RevertAid M-MuLV RT, oligo(dT)18 (cat. no. 639505; Takara, Dalian, China) in a 20-μl system according to the manufacturer's instructions. Reactions were incubated at 42˚C for 60 min, then 70˚C for 5 min and 16˚C hold. The thermal conditions for qPCR (Kapa Biosystems, Boston, MA, USA) were as follows: 95˚C for 5 min, followed by 40 cycles at 94˚C for 15 sec, 60˚C for 1 min and 70˚C 30 sec. The final extension step was 70˚C for 5 min and hold at 4˚C. β-actin was used as the internal control gene. The primer sequences were as follows: ALP, forward 5'-AAC CCAGACACAAGCATTCC-3', reverse 5'-GAGAGC GAAGGGTCAGTCAG-3'; OCN, forward 5'-TGCTTGTGA CGAGCTATCAG-3', reverse 5'-GAGGACAGGGAGGAT CAAGT-3'; Runx2, forward 5'-AAGTGCGGTGCAAAC TTTCT-3', reverse 5'-TCTCGGTGGCTGGTAGTGA-3'; Beclin 1 (BCN1), forward 5'-GTTGCCGTTATACTG TTCT-3' and reverse 5'-TTTCCACCTCTTCTTTGA-3' and β-actin forward, 5'-CCCATCTACGAGGGCTAT-3' and reverse, 5'-TGTCACGCACGATTTCC-3'. All reactions were performed in triplicate and the $2^{-\Delta\Delta Cq}$ method was used to quantify the results (22).

ALP activity assay. Before the cells were used for ALP activity assay and mineralization assay, they were cultured for a few days and the 6-well plates had a cell density of about $2.5x10^6$/well. ALP activity was measured by 5-bromo-4-chloro-3-indolyl phosphate (BCIP)/nitro blue tetrazolium (NBT) staining. Cells ($2x10^5$/well) cultured in 6-well plates (culture medium, 2 ml/well) were fixed with 4% paraformaldehyde and washed three times with double-distilled water, after which they were treated with BCIP/NBT solution (cat. no. C3206; Beyotime Institute of Biotechnology, Shanghai, China) for 30 min at 37˚C; staining images were then captured using an Olympus IX50 microscope (Olympus, Tokyo, Japan).

Mineralization assay. Cells ($2x10^5$/well) were rinsed three times with PBS and were fixed with 4% paraformaldehyde for 1 h at 4˚C, after which they were washed three times with double-distilled water and stained with 1% Alizarin red solution (pH 4.3) for 30 min at room temperature; the dye was removed with water. Images of the stained cells were then captured using an Olympus IX50 microscope (Olympus). For quantitative analysis, the stained cultures were destained with 100 mmol/l cetylpyridinium chloride for 1 h at room temperature. The absorbance of the released stain was measured at 550 nm and is presented relative to the control group.

Western blot analysis. Cells were rinsed three times with ice-cold PBS and were lysed in lysis buffer [30 mM Tris-HCl (pH 8.0), 150 mM NaCl, 1% NP-40; Bio-Swamp, Shanghai, China] containing 1 mM phenylmethylsulfonyl fluoride. Protein concentration was determined using a bicinchoninic acid assay (cat. no. P0009; Beyotime Institute of Biotechnology) assay. Protein samples (10 μg) were separated by 12% SDS-PAGE and electrotransferred to polyvinylidene difluoride membranes (EMD Millipore, Billerica, MA, USA). The membranes were blocked with 5% non-fat milk/Tris-buffered saline containing 0.05% Tween followed by incubation overnight at 4˚C with antibodies against total-AMPKα, p-AMPKα, p62 and LC3B (1:1,000 dilution). Appropriate peroxidase-conjugated secondary antibodies (goat anti-rabbit IgG; Bio-Swamp) were used to detect specific antibody binding. Protein bands were visualized using a chemiluminescence kit (cat. no. 32106; Thermo Fisher Scientific, Inc.) according to the manufacturer's protocol. ImageJ software version 1.48 (National Institutes of Health, Bethesda, MD, USA) was used to semi-quantify band intensity.

Silencing of BCN1. Small interfering (si)RNA targeting mouse BCN1 (siBCN1) and scrambled control siRNA (siControl) were chemically synthesized by Wuhan Myhalic Biotechnology Co., Ltd. (Wuhan, China). Cells were plated in 6-well plates at the density of $2x10^5$/well and cultured for 24 h in growth medium without antibiotics, after which they were transfected with siRNAs (30 nM) using Lipofectamine® 2000 reagent (cat. no. 11668027; Invitrogen; Thermo Fisher Scientific, Inc.) and cultured for 6 h at 37˚C. Subsequently, the medium was changed and RT-qPCR was performed 24, 48 and 72 h post-transfection, in order to assess the silencing effect; the most efficient siRNA was thus selected. A total of 24 h post-transfection using the selected siRNA, differentiation medium was added and the cells were treated with or without AICAR (10 μm) for 8 days at 37˚C. After 8 days, total RNA was collected from each group and RT-qPCR was performed to relatively quantify the expression levels of ALP, OCN and Runx2. In addition, ALP activity was assessed 8 days post-transfection. The siRNA sequences were as follows: siBCN1-I, sense 5'-GAUGGUGUC UCUCGAAGAUTT-3', antisense 5'-AUCUUCGAGAGACAC CAUCTT-3'; siBCN1-II, sense 5'-GGCACAAUCAAUAAU UUCATT-3', antisense 5'-UGAAAUUAUUGAUUGUGC CTT-3'; siBCN1-III, sense 5'-GGAGUGGAAUGAAAUCAA UTT, antisense 5'-AUUGAUUUCAUUCCACUCCTT-3'; and siControl, sense 5'-UUCUCCGAACGUGUCACGUTT-3' and

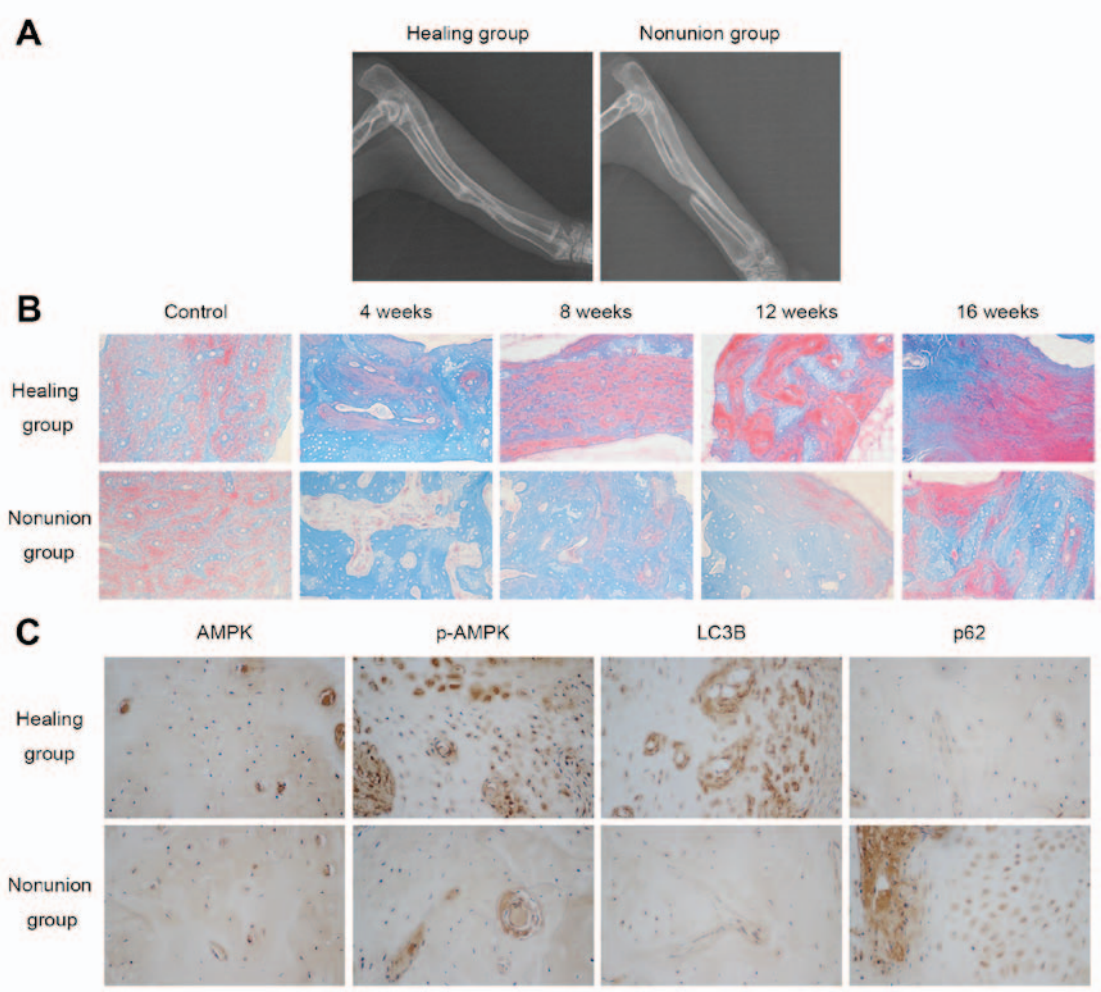

Figure 1. New bone mineralization and maturation is restrained in the nonunion group, accompanied by decreased AMPK activation and autophagic activity. (A) X-ray image showing the healing status of radial defects 16 weeks following surgery. (B) Masson staining (magnification, x200) detected osteoid (blue) and mineralized bone (red) in calluses obtained from normal bone (control) and fracture ends 4, 8, 12 and 16 weeks post-surgery. (C) Immunohistochemical staining of AMPK, p-AMPK and autophagy-associated markers (LC3B and p62) 4 weeks after surgery (magnification, x400). AMPK, adenosine monophosphate-activated protein kinase; LC3B, microtubule-associated proteins 1A/1B light chain 3B; p-AMPK, phosphorylated-AMPK.

antisense 5'-ACGUGACACGUUCGGAGAATT-3'. The silencing effect of the selected siRNA was verified by RT-qPCR and western blot analysis at 24, 48 and 72 h post-transfection.

Statistical analysis. All experiments were repeated at least three times and the results are expressed as the means ± standard error of the mean. The statistical analysis was performed using SPSS 19.0 software. The statistical analysis of differences between groups was evaluated by Student's t-test, or one-way analysis of variance followed by Fisher's least significant difference test. $P<0.05$ was considered to indicate a statistically significant difference.

Results

Radiographic and histological analysis of bone healing status in rabbits. A total of 16 weeks following surgery, the bilateral forelimbs of the rabbits in both groups were examined by radiography. As shown in Fig. 1A, rabbits in the healing group all achieved bony union in the radiuses, whereas nonunion was observed in the group that underwent 20 mm radial bone osteotomy, thus confirming the nonunion model had been successfully generated. Masson staining detected the maturation process of newly formed bone by staining osteoid and connective tissues blue, whereas mineralized bone was dyed red. The results indicated that new bone formation took place in both groups; however, the mineralization process of the healing group was more prominent and faster compared with in the nonunion group, as illustrated by a higher percentage of red staining at the same timepoints (4, 8, 12, 16 weeks post-operation) in the healing group (Fig. 1B). Collectively, these results suggested that new bone mineralization and maturation is restrained in the nonunion group.

Expression levels of AMPK and autophagy-associated markers in calluses. The present study examined the protein expression levels of AMPK, p-AMPK and autophagy-associated markers (LC3B and p62) in the calluses at various timepoints (4, 8, 12 and 16 weeks post-operation) by immunohistochemistry. As shown in Fig. 1C, there was no obvious difference in the expression of AMPK between the two groups 4 weeks after surgery, whereas p-AMPK and LC3B expression was higher, and p62 expression was lower in the healing group. With regards to other

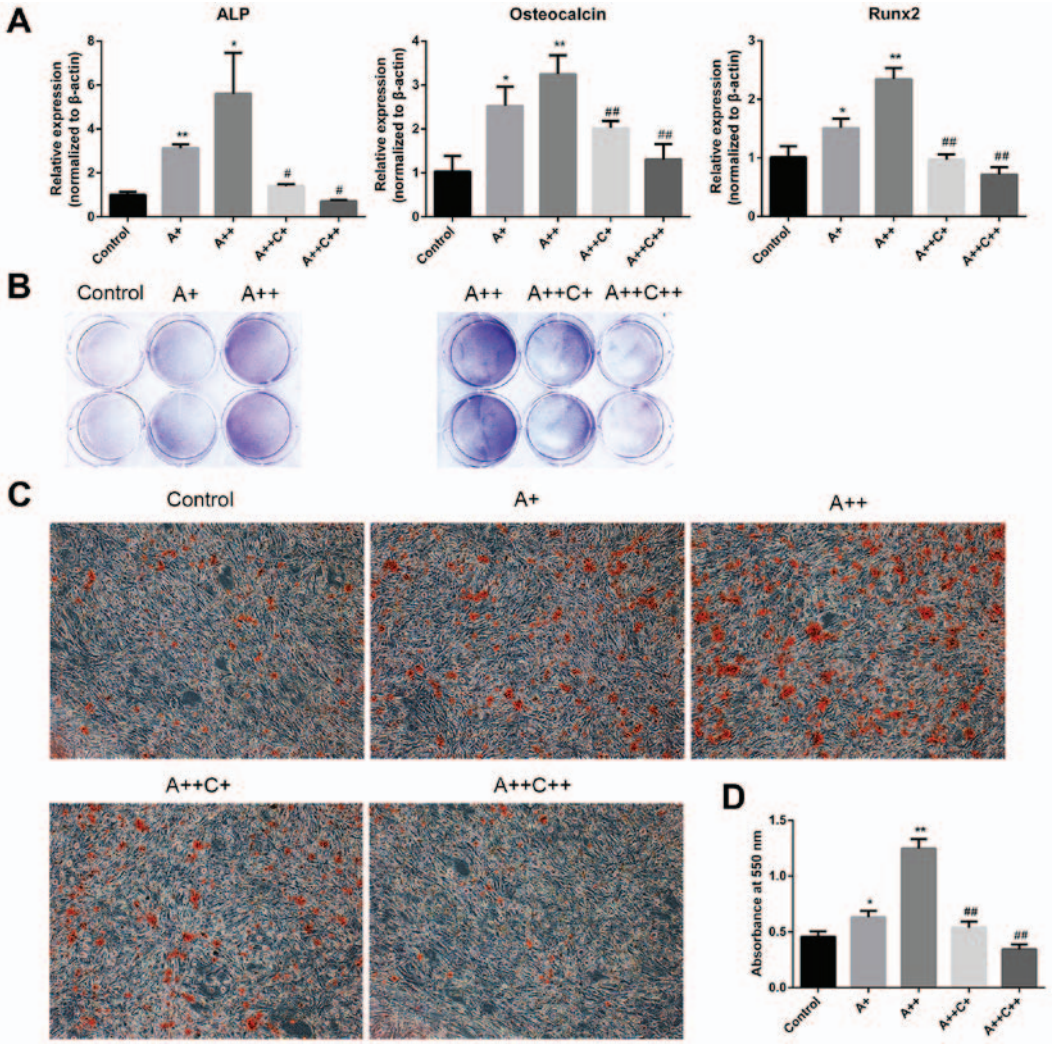

Figure 2. AMPK activation promotes the differentiation and mineralization of MC3T3-E1 cells. (A and B) Cells were treated with AICAR (A+, 1 μM; ++, 10 μM) and compound C (C+, 0.1 μM; ++, 1 μM) in differentiation medium for 8 days. (A) ALP, osteocalcin and Runx2 mRNA expression were detected by reverse transcription-quantitative polymerase chain reaction. (B) 5-Bromo-4-chloro-3-indolyl phosphate/nitro blue tetrazolium staining was used to determine ALP activity. (C) Cells were cultured for 21 days; representative images (magnification, x100) of mineralized nodules stained by Alizarin red staining are presented. (D) Quantification of Alizarin red staining with cetylpyridinium chloride. Absorbance was measured at 550 nm. *P<0.05, **P<0.01 compared with the control group; $^{\#}$P<0.05, $^{\#\#}$P<0.01 compared with the A++ group. AICAR, 5-aminoimdazole-4-carboxamide-1-β-D-ribofuranoside; ALP, alkaline phosphatase; AMPK, adenosine monophosphate-activated protein kinase; Rnx2, runt-related transcription factor 2.

time-points, no marked differences were detected between the groups. These results indicated that AMPK activation and autophagic activity were reduced in the nonunion group 4 weeks post-operation.

AMPK activation stimulates the osteogenic differentiation of MC3T3-E1 cells. ALP, OCN and Runx2 have been identified as typical markers of osteogenic differentiation (23). To investigate whether AMPK activation may stimulate the differentiation and mineralization of MC3T3-E1 cells, AICAR was added to the osteogenic differentiation medium in the presence or absence of compound C for 8 days, and the mRNA expression levels of ALP, OCN and Runx2 were assessed by RT-qPCR. In addition, ALP activity was detected by BCIP/NBT staining. Alizarin red staining was also applied to evaluate mineralization after 21 days of culture with the indicated treatment. AICAR significantly promoted the mRNA expression levels of ALP, OCN and Runx2 in a dose-dependent manner, whereas compound C, the AMPK inhibitor, reversed the effects of AICAR (Fig. 2A). In addition, BCIP/NBT staining indicated that AICAR enhanced ALP activity, whereas compound C suppressed the effects of AICAR in a dose-dependent manner (Fig. 2B). Furthermore, AICAR enhanced the mineralization of MC3T3-E1 cells, whereas compound C inhibited the effects of AICAR (Fig. 2C and D). Taken together, these results indicated that AMPK activation may promote the differentiation and mineralization of MC3T3-E1 osteoblasts.

AMPK activation induces autophagy in MC3T3-E1 cells. To determine whether AMPK activation induces autophagy, MC3T3-E1 cells were treated with AICAR for 24 h in the presence or absence of compound C; the protein expression levels of AMPK and p-AMPK, as well as the autophagy markers LC3B-I, LC3B-II and p62, were assessed by western blot analysis (Fig. 3A-D). Furthermore, autophagosomes were detected by transmission electron microscopy (Fig. 3E and F). Treatment with AICAR significantly stimulated activation of AMPK after 30 min of treatment; p-AMPK expression reached its peak after 24 h of

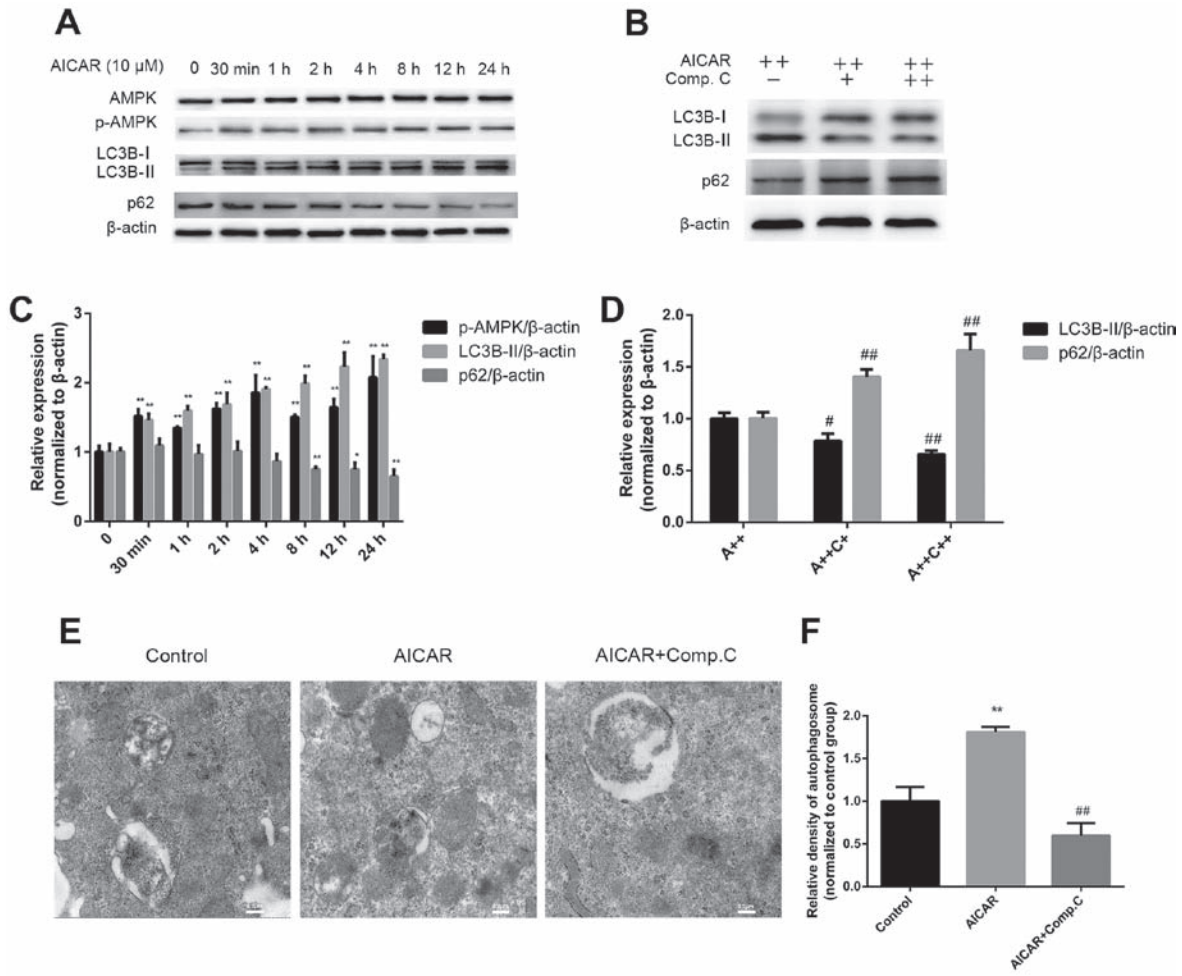

Figure 3. AMPK activation induces autophagy. (A) Cells were treated with AICAR and (B) AICAR (A++, 10 μM) + compound C (C++, 1 μM) for 24 h, after which western blot analysis was performed. (C and D) Semi-quantitative analysis of western blotting was conducted using ImageJ software and density values were normalized to β-actin, with the control group set as 1. (E) Cells were treated with AICAR (10 μM) or AICAR (10 μM) + compound C (1 μM) for 24 h. Representative images of autophagosomes were captured by transmission electron microscopy (scale bar, 0.2 μm). (F) Relative quantification of autophagosome density; values of the control group were set as 1. *P<0.05, **P<0.01 compared with the control group; $^{\#}$P<0.05, $^{\#\#}$P<0.01 compared with the AICAR(A++) group. AICAR, 5-aminoimdazole-4-carboxamide-1-β-D-ribofuranoside; AMPK, adenosine monophosphate-activated protein kinase; LC3B, microtubule-associated proteins 1A/1B light chain 3B; p-AMPK, phosphorylated-AMPK.

AICAR treatment. In addition, LC3B-II expression was increased after 30 min of AICAR treatment, whereas p62 expression was downregulated after 4 h; the lowest expression levels were detected at 24 h (Fig. 3A). Relative autophagosome density was higher following 24 h of AICAR treatment compared with in the control group (Fig. 3E and F). These results suggested that AICAR may stimulate AMPK activation and autophagy. To further confirm that AMPK activation by AICAR could induce autophagy, cells were incubated with AICAR for 24 h in combination with compound C, which is a specific AMPK inhibitor. As demonstrated in Fig. 3B, compound C markedly reduced LC3B-II expression, whereas p62 expression was increased. In addition, relative autophagosome density was markedly reduced by compound C compared with in the AICAR group. Taken together, these results indicated that AMPK activation may induce autophagy.

AMPK activation enhances differentiation and mineralization in MC3T3-E1 cells via the induction of autophagy. The aforementioned results demonstrated that AMPK activation could stimulate osteoblast differentiation and mineralization, during which autophagy was also induced. The present study subsequently examined whether the effects of AMPK activation on osteoblast differentiation and mineralization were mediated by autophagy induction. MC3T3-E1 cells were cotreated with AICAR and the following autophagy inhibitors: 3-MA, which suppresses initiation of autophagosome formation, and CQ, which inhibits the degradation of cargoes in the autophagosome, thus suppressing the final steps of autophagy. Western blot analysis verified the inhibition of autophagy by 3-MA and CQ (Fig. 4A and B). The results revealed that 3-MA and CQ markedly reduced ALP activity (Fig. 4C), and the mRNA expression levels of ALP, OCN and Runx2 in AICAR-treated cells (Fig. 4D). In addition, mineralization was suppressed by 3-MA and CQ compared with in cells treated with AICAR alone (Fig. 4E). To further confirm that the stimulatory effects of AMPK activation on osteoblast differentiation were due to autophagy, siRNA against BCN1 was used to more specifically inhibit autophagy. siBCN1-II was selected as the most efficient siRNA (Fig. 5A) and the silencing effect was confirmed by RT-qPCR and western blot analysis (Fig. 5B and C). As shown in Fig. 5D and E, ALP activity, and ALP, OCN and Runx2 mRNA expression were markedly decreased by siBCN1-II compared

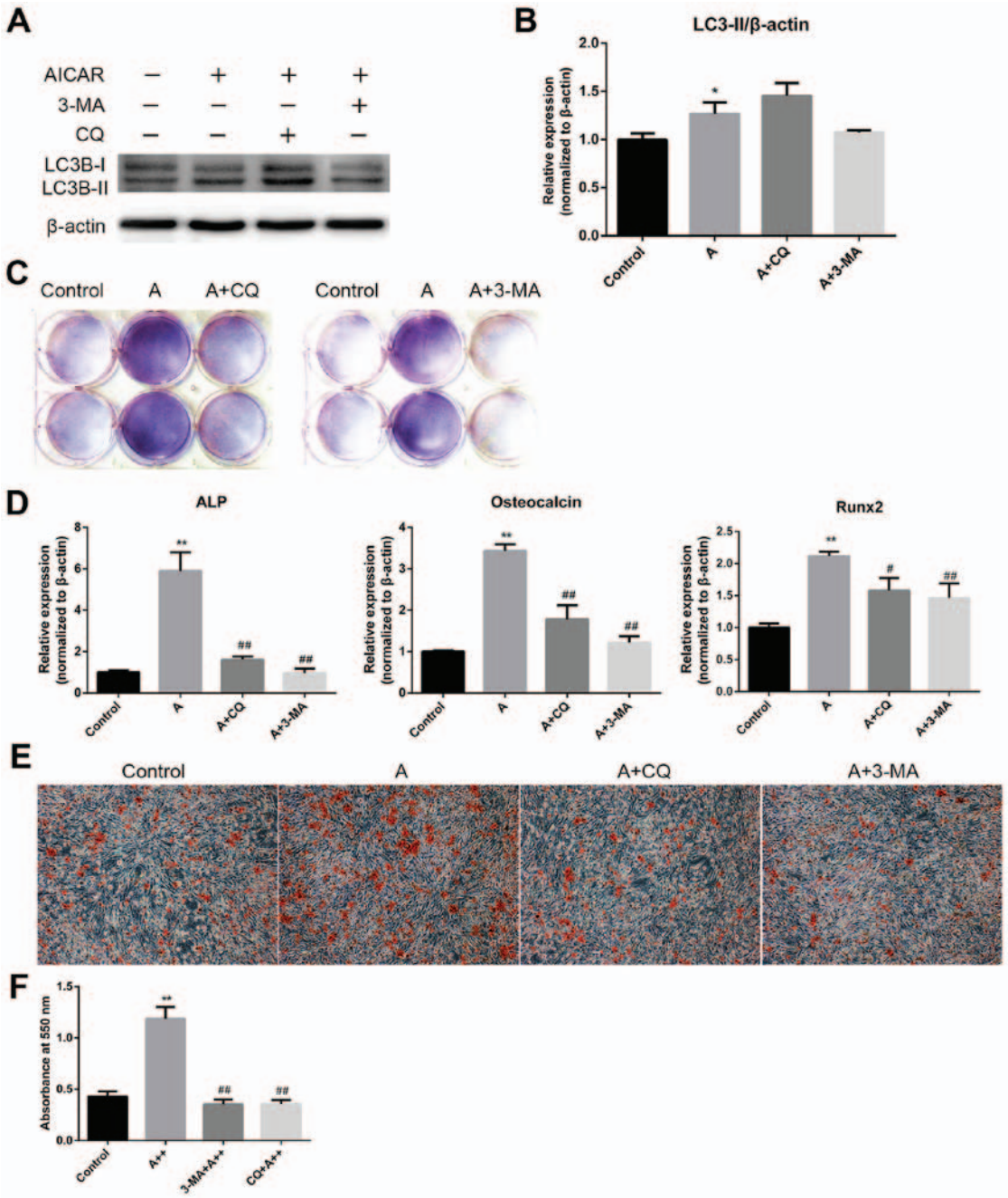

Figure 4. AMPK activation enhances differentiation and mineralization of MC3T3-E1 cells via the induction of autophagy. (A) Cells were treated with AICAR (10 μM) in the presence or absence of 3-MA (5 mM) or CQ (10 μM) for 24 h, after which western blot analysis was conducted. (B) Semi-quantitative results of western blot analysis. (C and D) Cells were cotreated with AICAR (10 μM) and 3-MA (5 mM) or CQ (10 μM) for 8 days. (C) 5-Bromo-4-chloro-3-indolyl phosphate/nitro blue tetrazolium staining was used to detect ALP activity. (D) ALP, OCN and Runx2 mRNA expression was detected using reverse transcription-polymerase chain reaction. (E) Cells were cultured for 21 days; representative images (magnification, x100) of Alizarin red staining are presented. (F) Quantification of Alizarin red staining. *P<0.05, **P<0.01 compared with the control group; $^{\#}$P<0.05, $^{\#\#}$P<0.01 compared with the AICAR(A++) group. 3-MA, 3-methyladenine; AICAR, 5-aminoimdazole-4-carboxamide-1-β-D-ribofuranoside; ALP, alkaline phosphatase; AMPK, adenosine monophosphate-activated protein kinase; CQ, chloroquine diphosphatase; OCN, osteocalcin; Runx2, runt-related transcription factor 2.

with in the AICAR group. Collectively, these results provide evidence to suggest that autophagy is involved in osteoblast differentiation and mineralization induced by AMPK activation.

Discussion

The results of the present study suggested that bone maturation is impaired in a rabbit model of nonunion, which was accompanied by decreased AMPK activation and autophagic activity in the early phase of fracture healing (4 weeks post-surgery). Furthermore, *in vitro* experiments indicated that AMPK activation induces autophagy, as well as osteoblast differentiation and mineralization, which can be reversed by the AMPK inhibitor compound C, by inhibition of autophagy with pharmacological inhibitors, or by BCN1 gene silencing. These results suggested that AMPK activation may promote osteoblast differentiation and mineralization via the induction of autophagy.

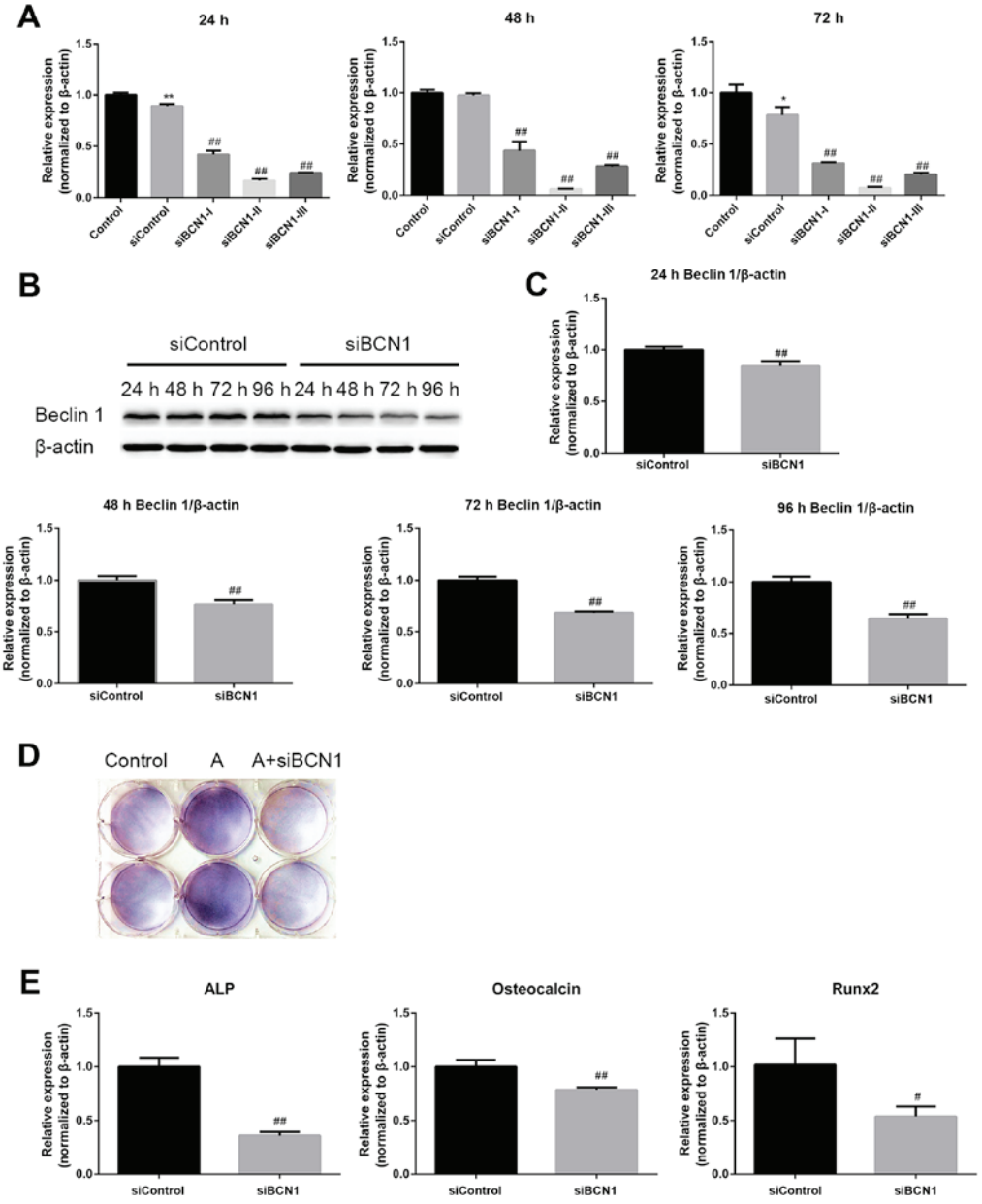

Figure 5. AMPK activation enhances differentiation of MC3T3-E1 cells via the induction of autophagy. (A) Cells were transfected with the indicated siRNAs, and the mRNA expression levels of BCN1 were measured by RT-qPCR 24, 48 and 72 h post-transfection to assess the silencing effect; siBCN1-II was the most efficient siRNA and was used for further study. (B) Cells were transfected with siBCN1-II and siControl, western blot analyis was performed using an antibody against BCN1 24, 48, 72 and 96 h post-transfection, in order to verify the silencing effect. (C) Semi-quantitative results of western blot analysis. (D and E) A total of 24 h post-transfection with siBCN1-II or siControl, differentiation medium was added and cells were treated with or without AICAR (10 μM) for 8 days. (D) 5-Bromo-4-chloro-3-indolyl phosphate/nitro blue tetrazolium staining was used to detect ALP activity. (E) ALP, OCN and Runx2 mRNA expression was detected by RT-PCR. siControl cells were treated with AICAR. *P<0.05, **P<0.01 compared with the control group; $^{\#}$P<0.05, $^{\#\#}$P<0.01 compared with the siControl group. AICAR, 5-aminoimdazole-4-carboxamide-1-β-D-ribofuranoside; ALP, alkaline phosphatase; AMPK, adenosine monophosphate-activated protein kinase; BCN1, Beclin 1; OCN, osteocalcin; Runx2, runt-related transcription factor 2; si/siRNA, small interfering RNA.

Osteoblasts, which are derived from mesenchymal precursor cells, are responsible for bone formation, and have a vital role in bone development and fracture repair (24). As osteoblasts differentiate, they secrete collagen and eventually form a mineralized extracellular matrix. Due to their increased expression during the differentiation process, ALP, OCN and Runx2 are widely used as markers to assess osteoblast differentiation (23). Osteoblast differentiation can be regulated by diverse molecules and signaling pathways, including Runx2, osterix, BMPs and Wnts (25,26). Agents capable of stimulating osteoblast differentiation have been reported to be beneficial for bone formation; for example, metformin and statins can stimulate bone formation by inducing BMP-2 and eNOS expression (27,28). Furthermore, drugs that target osteoblast differentiation to enhance bone formation have been applied in some clinical situations; for example, recombinant human-BMP-2 has been used to strengthen spinal fusion and BMP-7 has been used for the treatment of long-bone nonunion (25).

Nonunion refers to a situation where a bone fracture fails to heal over a prolonged period of time; it is not rare, with an overall incidence of 5-10% among patients with fractures (29).

Nonunion can be caused by numerous factors, including a large bone defect, infection, mechanical instability, soft tissue interposition, loss of vascularization and severe soft tissue damage (30-33). However, the underlying molecular mechanism remains elusive. Fracture healing is a complex physiological process in which several factors and cells interact in a coordinated manner (34). Osteoblasts have an essential role in new bone formation and bone remodeling by producing osteoid, which then becomes mineralized during the differentiation process (35). In the present study, radiographs captured 16 weeks post-operation detected nonunion in the nonunion group. Masson staining revealed that bone mineralization and maturation was markedly delayed in the nonunion group, which may be attributed to the prolonged existence of osteoid and impairment of the mineralization process. Based on these findings, it may be hypothesized that osteoblast differentiation is impaired in the development of nonunion.

AMPK has been recognized as a key energy sensor and metabolic modulator in regulating cell proliferation, differentiation, apoptosis, autophagy and mitochondrial function via various signaling pathways (36-38). It has been reported that activation of AMPK is able to stimulate osteoblast differentiation via eNOS and BMP-2 expression, as well as through the SMAD family member 1/5/8-Dlx5-Runx2 signaling pathway (10,28). Furthermore, AMPK activity has been reported to serve a crucial role in *in vitro* bone nodule formation and *in vivo* bone mass maintenance; knockout of AMPK gene expression may result in reduced cortical and trabecular bone parameters (8). The present results were in accordance with those of previous studies and indicated that activation of AMPK could enhance the differentiation and mineralization of MC3T3-E1 cells.

It has previously been demonstrated that autophagy is induced during the differentiation process of osteoblasts, and deficiencies in the expression of autophagy-essential genes may result in decreased mineralization capacity; furthermore, autophagic vacuoles may act as vehicles for the secretion of mineralization matrix (1). Notably, mechanical stress, which is an important stimulator for bone cells and can improve bone strength, has been revealed to be able to induce autophagy in osteoblasts; however, the process is transient (39,40). In line with these results, the present study indicated that autophagy was induced during AMPK-promoted MC3T3-E1 osteogenic differentiation, and inhibition of autophagy prevented the differentiation process.

A previous *in vitro* study demonstrated that a significant increase in osteoblast mineralization could be observed after 3-4 weeks cultivation (5). In addition, *in vivo* experiments revealed that hard callus and new bone formation could be detected in the margin of bone ends in rabbits 4 weeks after radius defect creation (41). The present results from immunohistochemical staining of AMPK, p-AMPK, LC3B and p62 in the calluses of fracture ends 4 weeks after surgery indicated that AMPK activity, as well as autophagy, was increased in the healing group compared with in the nonunion group. These events occurred at almost the same time period; therefore, considering the important role osteoblasts, AMPK and autophagy have in bone formation and remodeling, it may be hypothesized that AMPK and autophagy are involved in osteoblast differentiation, mineralization and the fracture healing process *in vivo*.

Inoki *et al* reported that AMPK may promote the initiation of autophagy via inhibition of mTOR (42). Furthermore, it has been revealed that AMPK may induce autophagy via direct phosphorylation of ULK1, which is essential in the initiation of autophagy (43). AMPK could also induce autophagy by directly phosphorylating the phosphatidylinositol 3-kinase catalytic subunit type 3 complex and BCN1, which are essential for autophagosome formation (44). Consistent with these results, the present study suggested that AMPK activation could induce autophagy in MC3T3-E1 cells.

The present study has some limitations. Firstly, the *in vivo* experiment was based on observation; agonists or inhibitors of AMPK and autophagy were not used to treat the animals, as there is insufficient evidence supporting the efficiency of these agents when applied *in vivo*. In addition, the signaling pathway by which AMPK activation induces autophagy and how autophagy stimulates osteoblast differentiation were not investigated; therefore, further research is required to elucidate these issues.

In conclusion, the results of the present study demonstrated that AMPK activation may stimulate osteoblast differentiation and mineralization through the induction of autophagy. In addition, AMPK activation and autophagy may be involved in the fracture healing process *in vivo*. The present study provides evidence to suggest that enhancing AMPK activation and autophagic activity may be a potential novel approach to promote fracture healing.

Acknowledgements

Not applicable.

Funding

The present study was supported by the Hubei Provincial Natural Science Foundation of China (grant nos. 2015CFB209); the Fundamental Research Funds for the Central Universities (grant no. 2042015kf0070); and the Zhongnan Hospital of Wuhan University Science, Technology and Innovation Seed Fund, Project znpy2016004.

Availability of data and materials

Materials described in the manuscript, including all relevant raw data, will be freely available to any researcher wishing to use them for non-commercial purposes, without breaching participant confidentiality.

Authors' contributions

YL wrote the manuscript. YL, JS and WS performed the experiments. LC and ZD designed the study and reviewed the manuscript. All authors read and approved the manuscript.

Ethics approval and consent to participate

The present study was approved by the Wuhan University Zhongnan Hospital Research Committee (Wuhan, China).

Consent for publication

Not applicable.

Competing interests

The authors declare that they have no competing interests.

References

1. Nollet M, Santucci-Darmanin S, Breuil V, Al-Sahlanee R, Cros C, Topi M, Momier D, Samson M, Pagnotta S, Cailleteau L, *et al*: Autophagy in osteoblasts is involved in mineralization and bone homeostasis. Autophagy 10: 1965-1977, 2014.
2. Chan GK and Duque G: Age-related bone loss: old bone, new facts. Gerontology 48: 62-71, 2002.
3. Homma Y, Zimmermann G and Hernigou P: Cellular therapies for the treatment of non-union: the past, present and future. Injury 44 (Suppl 1): S46-S49, 2013.
4. Zhu Y, Zhou J, Ao R and Yu B: A-769662 protects osteoblasts from hydrogen dioxide-induced apoptosis through activating of AMP-activated protein kinase (AMPK). Int J Mol Sci 15: 11190-11203, 2014.
5. Quarles LD, Yohay DA, Lever LW, Caton R and Wenstrup RJ: Distinct proliferative and differentiated stages of murine MC3T3-E1 cells in culture: an in vitro model of osteoblast development. J Bone Miner Res 7: 683-692, 1992.
6. Zhong X, Xiu LL, Wei GH, Liu YY, Su L, Cao XP, Li YB and Xiao HP: Bezafibrate enhances proliferation and differentiation of osteoblastic MC3T3-E1 cells via AMPK and eNOS activation. Acta Pharmacol Sin 32: 591-600, 2011.
7. Hardie DG, Hawley SA and Scott JW: AMP-activated protein kinase - development of the energy sensor concept. J Physiol 574: 7-15, 2006.
8. Shah M, Kola B, Bataveljic A, Arnett TR, Viollet B, Saxon L, Korbonits M and Chenu C: AMP-activated protein kinase (AMPK) activation regulates in vitro bone formation and bone mass. Bone 47: 309-319, 2010.
9. Mihaylova MM and Shaw RJ: The AMPK signalling pathway coordinates cell growth, autophagy and metabolism. Nat Cell Biol 13: 1016-1023, 2011.
10. Jang WG, Kim EJ, Lee KN, Son HJ and Koh JT: AMP-activated protein kinase (AMPK) positively regulates osteoblast differentiation via induction of Dlx5-dependent Runx2 expression in MC3T3E1 cells. Biochem Biophys Res Commun 404: 1004-1009, 2011.
11. Kanazawa I, Yamaguchi T, Yano S, Yamauchi M and Sugimoto T: Activation of AMP kinase and inhibition of Rho kinase induce the mineralization of osteoblastic MC3T3-E1 cells through endothelial NOS and BMP-2 expression. Am J Physiol Endocrinol Metab 296: E139-E146, 2009.
12. Pierrefite-Carle V, Santucci-Darmanin S, Breuil V, Camuzard O and Carle GF: Autophagy in bone: self-eating to stay in balance. Ageing Res Rev 24 (Pt B): 206-217, 2015.
13. Mizushima N, Levine B, Cuervo AM and Klionsky DJ: Autophagy fights disease through cellular self-digestion. Nature 451: 1069-1075, 2008.
14. Hosokawa N, Sasaki T, Iemura S, Natsume T, Hara T and Mizushima N: Atg101, a novel mammalian autophagy protein interacting with Atg13. Autophagy 5: 973-979, 2009.
15. Mercer CA, Kaliappan A and Dennis PB: A novel, human Atg13 binding protein, Atg101, interacts with ULK1 and is essential for macroautophagy. Autophagy 5: 649-662, 2009.
16. Glick D, Barth S and Macleod KF: Autophagy: cellular and molecular mechanisms. J Pathol 221: 3-12, 2010.
17. National Research Council (US) Committee for the Update of the Guide for the Care and Use of Laboratory Animals: Guide for the care and use of laboratory animals. 8th edition. Washington (DC): National Academies Press (US); 2011.
18. Farso Nielsen F, Karring T and Gogolewski S: Biodegradable guide for bone regeneration. Polyurethane membranes tested in rabbit radius defects. Acta Orthop Scand 63: 66-69, 1992.
19. Shafiei Z, Bigham AS, Dehghani SN and Nezhad ST: Fresh cortical autograft versus fresh cortical allograft effects on experimental bone healing in rabbits: radiological, histopathological and biomechanical evaluation. Cell Tissue Bank 10: 19-26, 2009.
20. Oryan A, Alidadi S and Moshiri A: Current concerns regarding healing of bone defects. Hard Tissue 2: 13, 2013.
21. Saito T, Asai K, Sato S, Hayashi M, Adachi A, Sasaki Y, Takano H, Mizuno K and Shimizu W: Autophagic vacuoles in cardiomyocytes of dilated cardiomyopathy with initially decompensated heart failure predict improved prognosis. Autophagy 12: 579-587, 2016.
22. Livak KJ and Schmittgen TD: Analysis of relative gene expression data using real-time quantitative PCR and the 2(-Delta Delta C(T)) Method. Methods 25: 402-408, 2001.
23. Aubin JE, Liu F, Malaval L and Gupta AK: Osteoblast and chondroblast differentiation. Bone 17 (Suppl 2): 77S-83S, 1995.
24. Shapiro F: Bone development and its relation to fracture repair. The role of mesenchymal osteoblasts and surface osteoblasts. Eur Cell Mater 15: 53-76, 2008.
25. Khosla S, Westendorf JJ and Oursler MJ: Building bone to reverse osteoporosis and repair fractures. J Clin Invest 118: 421-428, 2008.
26. Nakashima K and de Crombrugghe B: Transcriptional mechanisms in osteoblast differentiation and bone formation. Trends Genet 19: 458-466, 2003.
27. Garrett IR, Gutierrez G and Mundy GR: Statins and bone formation. Curr Pharm Des 7: 715-736, 2001.
28. Kanazawa I, Yamaguchi T, Yano S, Yamauchi M and Sugimoto T: Metformin enhances the differentiation and mineralization of osteoblastic MC3T3-E1 cells via AMP kinase activation as well as eNOS and BMP-2 expression. Biochem Biophys Res Commun 375: 414-419, 2008.
29. Gómez-Barrena E, Rosset P, Lozano D, Stanovici J, Ermthaller C and Gerbhard F: Bone fracture healing: cell therapy in delayed unions and nonunions. Bone 70: 93-101, 2015.
30. Altner PC, Grana L and Gordon M: An experimental study on the significance of muscle tissue interposition on fracture healing. Clin Orthop Relat Res 111: 269-273, 1975.
31. Heiple KG and Herndon CH: The pathologic physiology of nonunion. Clin Orthop Relat Res 43: 11-21, 1965.
32. Hietaniemi K, Peltonen J and Paavolainen P: An experimental model for non-union in rats. Injury 26: 681-686, 1995.
33. Sarahrudi K, Mousavi M, Grossschmidt K, Sela N, König F, Vécsei V and Aharinejad S: Combination of anorganic bovine-derived hydroxyapatite with binding peptide does not enhance bone healing in a critical-size defect in a rabbit model. J Orthop Res 26: 759-763, 2008.
34. Tsiridis E, Upadhyay N and Giannoudis P: Molecular aspects of fracture healing: which are the important molecules? Injury 38 (Suppl 1): S11-S25, 2007.
35. Harada S and Rodan GA: Control of osteoblast function and regulation of bone mass. Nature 423: 349-355, 2003.
36. Steinberg GR and Kemp BE: AMPK in health and disease. Physiol Rev 89: 1025-1078, 2009.
37. Greer EL, Oskoui PR, Banko MR, Maniar JM, Gygi MP, Gygi SP and Brunet A: The energy sensor AMP-activated protein kinase directly regulates the mammalian FOXO3 transcription factor. J Biol Chem 282: 30107-30119, 2007.
38. Wang S, Song P and Zou MH: AMP-activated protein kinase, stress responses and cardiovascular diseases. Clin Sci (Lond) 122: 555-573, 2012.
39. King JS, Veltman DM and Insall RH: The induction of autophagy by mechanical stress. Autophagy 7: 1490-1499, 2011.
40. Klein-Nulend J, Bacabac RG and Bakker AD: Mechanical loading and how it affects bone cells: the role of the osteocyte cytoskeleton in maintaining our skeleton. Eur Cell Mater 24: 278-291, 2012.
41. Zhao L, Zhao J, Wang S, Wang J and Liu J: Comparative study between tissue-engineered periosteum and structural allograft in rabbit critical-sized radial defect model. J Biomed Mater Res B Appl Biomater 97: 1-9, 2011.
42. Inoki K, Zhu T and Guan KL: TSC2 mediates cellular energy response to control cell growth and survival. Cell 115: 577-590, 2003.
43. Egan DF, Shackelford DB, Mihaylova MM, Gelino S, Kohnz RA, Mair W, Vasquez DS, Joshi A, Gwinn DM, Taylor R, *et al*: Phosphorylation of ULK1 (hATG1) by AMP-activated protein kinase connects energy sensing to mitophagy. Science 331: 456-461, 2011.
44. Kim J, Kim YC, Fang C, Russell RC, Kim JH, Fan W, Liu R, Zhong Q and Guan KL: Differential regulation of distinct Vps34 complexes by AMPK in nutrient stress and autophagy. Cell 152: 290-303, 2013.